Inorganic Chemistry
Article

Weak Metamagnetic-like 1D Manganese(II) Complex with a Double $\mu_{1,1}$-Azido Bridge: A Structure and Magnetic Study

Anamika Das,[†] Georgina M. Rosair,[‡] M. Salah El Fallah,*,[§] Joan Ribas,[§] and Samiran Mitra*,[†]

Department of Chemistry, Jadavpur University, Kolkata 700032, India, Department of Chemistry, Heriot-Watt University, Edinburg EH14 4AS, U.K., and Departament de Química Inorgànica, Universitat de Barcelona, Martí i Franquès 1–11, Barcelona 08028, Spain

The azido-bridged manganese complex of formula [Mn(tptz)($\mu_{1,1}$-N$_3$)$_2$]$_n$ [**1**; tptz = 2,4,6-tris(2-pyridyl)-1,3,5-triazine] has been synthesized and characterized by single-crystal X-ray diffraction analysis and a low-temperature magnetic study. The complex **1** crystallizes in the orthorhombic space group *Pbcn*, with a = 17.911(5) Å, b = 15.804(5) Å, c = 6.6538(18) Å, and Z = 4. The Mn atoms are coordinated by three N atoms of the tptz ligands and connected to each other by double end-on (EO) azide ligands, forming a neutral 1D chain. The adjacent 1D chains are connected by face-to-face π–π-stacking interactions and C–H$\cdots\pi$ interactions of pyridine rings of the tptz ligands, which leads to the formation of a supramolecular 2D sheet structure. Temperature- and field-dependent magnetic analyses reveal dominant intrachain ferromagnetic interactions with EO azide-bridge and weak interchain antiferromagnetic interactions with overall metamagnetic behavior having 3D magnetic ordering at 2.7 K. The critical field is approximately 80 G, at which the interlayer antiferromagnetic ground-state switches to a ferromagnetic state.

Introduction

During the past decades, scientists have been engaged in the synthesis of new molecule-based magnets, i.e., compounds with strong molecular character exhibiting spontaneous magnetization below a certain critical temperature.[1–3] Molecule-based magnets exhibit a wide variety of bonding and structural motifs. These include one-, two-, and three-dimensional (1D, 2D, and 3D, respectively) network structures by variation of metal atoms and ligands.[4,5] The contemporary challenge to the synthetic inorganic chemists is to produce new compounds with preassigned magnetic properties and, for this, the rational synthetic design for the tuning of the solid-state structure is important. Among the large number of bridging ligands, the azide ion can act as an efficient and versatile magnetic coupler[6] owing to its

* To whom correspondence should be addressed: E-mail: smitra_2002@yahoo.com (S.M.), salah.elfallah@qi.ub.es (M.S.E.F.). Fax: 91-33-2414-6414 (S.M.).
 † Jadavpur University.
 ‡ Heriot-Watt University.
 § Universitat de Barcelona.

 (1) (a) Tasiopoulos, A. T.; Vinslava, A.; Wernsdorfer, W.; Abboud, K. A.; Christou, G. *Angew. Chem., Int. Ed.* **2004**, *43*, 2117. (b) Gatteschi, D.; Sessoli, R. *Angew. Chem., Int. Ed.* **2003**, *42*, 268. (c) Brechin, E. K.; Boskovic, C.; Wernsdorfer, W.; Yoo, J.; Yamaguchi, A.; Sañudo, E. C.; Concolino, T. R.; Rheingold, A. L.; Ishimoto, H.; Hendrickson, D. N.; Christou, G. *J. Am. Chem. Soc.* **2002**, *124*, 9710. (d) Boudalis, A. K.; Donnadieu, B.; Nastopoulos, V.; Clemente-Juan, J. M.; Mari, A.; Sanakis, Y.; Tuchagues, J.-P.; Perlepes, S. P. *Angew. Chem., Int. Ed.* **2004**, *43*, 2266.
 (2) (a) Holmes, S. M.; Girolami, G. S. *J. Am. Chem. Soc.* **1999**, *121*, 5593. (b) Verdaguer, M. *Science* **1996**, *272*, 698. (c) Sessoli, R.; Tsai, H. L.; Schake, A. R.; Wang, S. Y.; Vincent, J. B.; Folting, K. Gatteschi, D.; Christou, G.; Hendrickson, D. N. *J. Am. Chem. Soc.* **1993**, *115*, 1804.

 (3) (a) *Magnetism: Molecules to Materials*; Miller, J. S., Drilon, M., Eds.; Wiley-VCH: Weinheim, Germany, 2002; Vol. 3. (b) Kahn, O. *Molecular Magnetism*; VCH: Weinheim, Germany, 1993. (c) *Magneto Structural Correlations in Exchange Coupled Systems*; Willet, R. D., Gatteschi, D., Kahn, O., Eds.; NATO Advanced Study Institute Series C140; Reidel: Dordrecht, The Netherlands, 1985. (d) Miller, J. S.; Epestein, A. J.; Reiff, W. M. *Science* **1988**, *240*, 40.
 (4) (a) Ohba, M.; Ōkawa, H. *Coord. Chem. Rev.* **2000**, *198*, 313. (b) Li, D.; Zheng, L.; Zhang, Y.; Huang, J.; Gao, S.; Tang, W. *Inorg Chem.* **2003**, *42*, 6123. (c) Zeng, M.-H.; Zhang, W.-X.; Sun, X.-Z.; Chen, X.-M. *Angew. Chem., Int. Ed.* **2005**, *44*, 3079. (d) Li, D.-F.; Zheng, L.-M.; Wang, X.-Y.; Huang, J.; Gao, S.; Tang, W.-X. *Chem. Mater.* **2003**, *15*, 2094.
 (5) (a) Maji, T. K.; Kaneko, W.; Ohba, M.; Kitagawa, S. *Chem. Commun.* **2005**, 4613. (b) Ghoshal, D.; Maji, T. K.; Mostafa, G.; Sain, S.; Lu, T.-H.; Ribas, J.; Zangrando, E.; Chaudhuri, R. N. *Dalton Trans.* **2004**, 1687. (c) Dey, S. K.; Bag, B.; Malik, K. M. A.; El Fallah, M. S.; Ribas, J.; Mitra, S. *Inorg. Chem.* **2003**, *42*, 4029. (d) Casarin, M.; Corvaja, C.; Di Nicola, C.; Falcomer, D.; Franco, L.; Monari, M.; Pandolfo, L.; Pettinari, C.; Piccinelli, F. *Inorg Chem.* **2005**, *44*, 6265.
 (6) (a) Ribas, J.; Escuer, A.; Monfort, M.; Vicente, R.; Cortés, R.; Lezama, L.; Rojo, T. *Coord. Chem. Rev.* **1999**, *193–195*, 1027. (b) Ruiz, E.; Cano, J.; Alvarez, S.; Alemany, P. *J. Am. Chem. Soc.* **1998**, *120*, 11122.

Chart 1

End-on (1,1)   **End to end(1,3)**
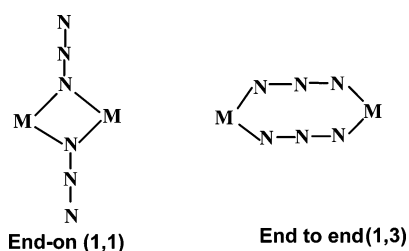
different bridging modes, either in $\mu_{1,1}$ (end-on, EO) or in $\mu_{1,3}$ (end-to-end, EE) (Chart 1). The literature search indicates that a considerable number of works have been reported concerning the versatility of the azide ion.[7−13] From the magnetic point of view, the coordination modes of the azide ligands greatly affect the nature and magnitude of the magnetic exchange interaction in these polynuclear azide complexes. It is well established that the complexes with double symmetric EE bridges produce antiferromagnetic coupling,[9] whereas symmetric EO bridges usually exhibit ferromagnetic coupling.[10] Furthermore, EE and EO bridging modes may simultaneously exist in the same species, leading to different topologies and magnetic properties.[11−13] In addition, the judicial choice of the metal atoms along with

the bridging ligands is also an important factor. Among the first-row transition-metal azides, the exchange interaction between the high-spin Mn^{II} centers is desirable because this ion contains the highest possible number of unpaired electrons. Apart from these, different organic molecules that are used as coligands and countercations present other than the metal atoms may also sometime influences the intra- and interlayer structure and hence the magnetic properties.[5a,14]

Thus, in our continuous search toward molecule-based magnets, we select 2,4,6-tris(2-pyridyl)-1,3,5-triazine (tptz) as a coligand and observe the behavior of this particular ligand over a Mn−azide system. Here in this paper, we present the synthesis and characterization of a new polymeric Mn−azide complex, $[Mn(tptz)(\mu_{1,1}\text{-}N_3)_2]_n$ (**1**), which is characterized by single-crystal X-ray diffraction and low-temperature magnetic studies. Here each Mn^{II} is seven-coordinated and is connected to one another by a double EO bridging azide ligand, forming a 1D chain. The adjacent 1D chains are connected by face-to-face $\pi-\pi$-stacking interactions and C−H···π interactions of the pyridine rings of the tptz ligand, which leads to the formation of a supramolecular 2D sheet. Variable-temperature magnetic measurement exhibits intrachain ferromagnetic interactions and interchain antiferromagnetic interactions with the overall metamagnetic behavior having 3D magnetic ordering at 2.7 K.

Experimental Section

Materials. High-purity (98%) 2,4,6-tris(2-pyridyl)-1,3,5-triazine (tptz) was purchased from the Aldrich Chemical Co. Inc. and used without further purification. All other chemicals were of analytical reagent grade.

Caution! Perchlorate salts and azido complexes are potentially explosive in the presence of organic compounds. Only a small amount of the materials should be prepared and handled with care.

Physical Measurements. Elemental analyses were carried out using a Perkin-Elmer 2400 II elemental analyzer. The IR spectrum was recorded on a Perkin-Elmer 883-IR spectrophotometer using KBr pellets. The magnetic measurements were carried out on a polycrystalline sample using a Quantum Design SQUID MPMS-XL magnetometer in the temperature range of 2−300 K with an applied field of 3000 G. The contribution of the sample holder was determined separately in the same temperature range and field. Diamagnetic corrections were estimated from Pascal's constants.[3b]

Synthesis of $[Mn(tptz)(\mu_{1,1}\text{-}N_3)_2]_n$ (1). A methanolic solution (10 mL) of tptz (0.156 g, 0.5 mmol) was slowly added to an aqueous solution of $Mn(ClO_4)_2\cdot6H_2O$ (0.182 g, 0.5 mmol). The solution was stirred for few minutes at room temperature. Then an aqueous solution of NaN_3 (0.0650 g, 1 mmol) was added to this solution dropwise with constant stirring. The deep-yellow solution was filtered off, and the filtrate was kept at room temperature. After 4 days, orange block-shaped crystals, suitable for X-ray diffraction, were obtained from the filtrate. Yield: 90%. Anal. Calcd for $C_{18}H_{12}$-MnN_{12}: C, 47.85; H, 2.65; N, 37.22. Found: C, 47.65; H, 2.92; N, 37.25.

(7) (a) Abu-Youssef, M. A. M.; Escuer, A.; Goher, M. A. S.; Mautner, F. A.; Vicente, R. *J. Chem. Soc., Dalton Trans*. **2000**, 413. (b) Abu-Youssef, M. A. M.; Escuer, A.; Goher, M. A. S.; Mautner, F. A.; Vicente, R. *Eur. J. Inorg. Chem.* **1999**, 687. (c) Escuer, A.; Vicente, R.; Goher, M. A. S.; Mautner, F. A. *Inorg. Chem.* **1998**, *37*, 782. (d) Cortes, R.; Drillon, M.; Solans, X.; Lezama, L.; Rojo, T. *Inorg. Chem.* **1997**, *36*, 677.

(8) (a) Xie, Y.; Liu, Q.; Jiang, H.; Du, C.; Xu, X.; Yu, M.; Zhu, Yu. *New J. Chem.* **2002**, *26*, 176. (b) Ray, M. S.; Ghosh, A.; Bhattacharya, R.; Mukhopadhyay, G.; Drew, M. G.; Ribas, J. *Dalton Trans.* **2004** 252.

(9) (a) Ni, Z.-H.; Kou, H.-Z.; Zheng, L.; Zhao, Y.-H.; Zhang, L.-F.; Wang, R.-J.; Cui, A.-L.; Sato, O. *Inorg. Chem.* **2005**, *44*, 4728. (b) Mukherjee, P. S.; Maji, T. K.; Escuer, A.; Vicente, R.; Ribas, J.; Rosair, G.; Mautner, F. A.; Chaudhuri, R. N. *Eur. J. Inorg. Chem.* **2002**, *4*, 943. (c) Escuer, A.; Vicente, R.; El Fallah, M. S.; Solans, X.; Font-Bardia, M. *Inorg. Chim. Acta* **1998**, *278*, 43. (d) Shen, H.-Y.; Liao, D.-Z.; Jiang, Z.-H.; Yan, S.-P.; Sun, B.-W.; Wang, G.-L.; Yao, X.-K.; Wang, H.-G. *Chem. Lett.* **1998**, *5*, 469. (e) Escuer, A.; Castro, I.; Mautner, F.; El Fallah, M. S.; Vicente, R. *Inorg. Chem.* **1997**, *36*, 4633.

(10) Gao, E.-Q.; Cheng, A.-L.; Xu, Y.-X.; He, M.-Y.; Yan, C.-H. *Inorg. Chem.* **2005**, *44*, 8822. (b) Dey, S. K.; Mondal, N.; El Fallah, M. S.; Vicente, R.; Escuer, A.; Solans, X.; Bardia, M. F.; Matsushita, T.; Gramlich, V.; Mitra, S. *Inorg. Chem.* **2004**, *43*, 2427. (c) Barandika, M. G.; Cortes, R.; Lezama, L.; Urtiaga, M. K.; Arriortua, M. I.; Rojo, T. *J. Chem. Soc., Dalton Trans.* **1999**, 2971. (d) Rajendiran, T. M.; Mathoniere, C.; Golhen, S.; Ouahab, L.; Kahn, O. *Inorg. Chem.* **1998**, *37*, 2651. (e) Escuer, A.; Vicente, R.; Ribas, J.; Solans, X. *Inorg. Chem.* **1995**, *34*, 1793.

(11) (a) Ghosh, A K.; Ghoshal, D.; Zangrando, E.; Ribas, J.; Chaudhuri, R. N. *Inorg. Chem.* **2005**, *44*, 1786. (b) Gao, E.-Q.; Yue, Y.-F.; Bai, S.-Q.; He, Z.; Zhang, S.-W.; Yan, C.-H. *Chem. Mater.* **2004**, *16*, 1590. (c) Gao, E.-Q.; Bai, S.-Q.; Wang, C.-F.; Yue, Y.-F.; Yan, C.-H. *Inorg. Chem.* **2003**, *42*, 8456. (d) Escuer, A.; Cano, J.; Goher, M. A. S.; Journaux, Y.; Lloret, F.; Mautner, F. A.; Vicente, R. *Inorg. Chem.* **2000**, *39*, 4688 and references cited therein. (e) Viau, G.; Lombardi, M. G.; De Munno, G.; Julve, M.; Lloret, F.; Faus, J.; Caneschi, A.; Clemente-Juan, J. M. *Chem. Commun.* **1997**, 1195.

(12) (a) Escuer, A.; Mautner, F. A.; Goher, M. A. S.; Abu-Youssef, M. A. M.; Vicente, R. *Chem. Commun.* **2005**, 605. (b) Gao, E. Q.; Yue, Y. F.; Bai, S. Q.; He, Z.; Yan, C. H. *J. Am. Chem. Soc.* **2004**, *126*, 1419. (c) Wen, H.-R.; Wang, C.-F.; Song, Y.; Zuo, J.-L.; You, X.-Z. *Inorg. Chem.* **2005**, *44*, 9039.

(13) (a) Monfort, M.; Resino, I.; Ribas, J.; Evans, H. S. *Angew. Chem., Int. Ed.* **2000**, *39*, 191. (b) Gao, E.-Q.; Wang, Z.-M.; Yan, C.-H. *Chem. Commun.* **2003**, 1748. (c) Rujiwatra, A.; Kepert, C. J.; Claridge, J. B.; Rosseinsky, M. J.; Kumagai, H.; Kurmoo, M. *J. Am. Chem. Soc.* **2001**, *123*, 10584. (d) Zeng, M.-H.; Zhang, W.-X.; Sun, X.-Z.; Chen, X.-M. *Angew. Chem., Int. Ed.* **2005**, *44*, 3079.

(14) (a) Goher, M. A. S.; Cano, J.; Journaux, Y.; Abu-Youssef, M. A. M.; Mautner, F. A.; Escuer, A.; Vicente, R. *Chem.—Eur. J.* **2000**, *6*, 778. (b) Ribas, J.; Monfort, M.; Solans, X.; Drillon, M. *Inorg. Chem.* **1994**, *33*, 742. (c) Mautner, F. A.; Cortes, R.; Lezama, L.; Rojo, T. *Angew. Chem., Int. Ed. Engl.* **1996**, *35*, 78.

Table 1. Crystal Data and Structure Refinements of Complex **1**

empirical formula	$C_{18}H_{12}MnN_{12}$
fw	451.34
cryst syst	orthorhombic
space group	*Pbcn* (No. 60)
a (Å)	17.911(5)
b (Å)	15.804(5)
c (Å)	6.6538(18)
V (Å^3)	1883.5(9)
Z	4
temperature (K)	100
$\lambda_{Mo\ K\alpha}$ (Å)	0.710 73
D_c (g cm^{-3})	1.592
μ (mm^{-1})	0.737
F(000)	916
θ range (deg)	2.3−34.8
total data	29412
unique data	4030
obsd data [$I > 2\sigma(I)$]	2361
N_{ref}, N_{par}	4030, 143
GOF	0.95
R^a	0.0429
R_w^b	0.1011
R_{int}	0.055
$\Delta\rho_{max}$ (e Å^{-3})	0.64
$\Delta\rho_{min}$ (e Å^{-3})	−0.79

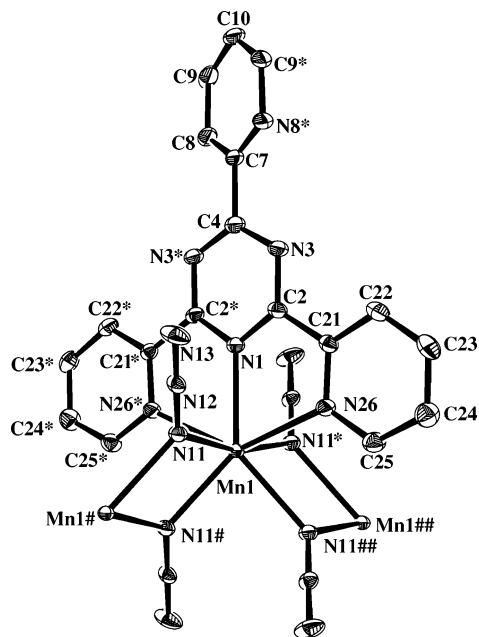$^a R = \sum(|F_o - F_c|)/\sum|F_o|.$ $^b R_w = \{\sum[w(|F_o - F_c|)^2]/\sum[w|F_o|^2]\}^{1/2}.$

Crystallographic Data Collection and Refinement. Crystal data, details of the collection, and refinements for the structure are summarized in Table 1. The data collection for complex **1** was carried out at 100 K on a Bruker X8 Apex2 diffractometer equipped with a graphite monochromator and Mo Kα ($\lambda = 0.710\ 73$ Å) radiation. The structure was solved by direct methods, followed by successive Fourier and difference Fourier syntheses and refined by full-matrix least squares on F^2. All non-H atoms were refined with anisotropic displacement parameters, and H atoms are placed geometrically followed by refinement with riding isotropic displacement parameters. C8 and N8 are superimposed on each other by crystallographic symmetry so this site was refined as 50% C and 50% N with tied displacement parameters and coordinates. All of the crystallographic computations were carried out using *SHELXTL*, *PLATON 99*,[15] and ORTEP programs.[16]

Results and Discussion

IR Spectroscopy. Complex **1** shows two intense absorption bands at 2066 and 2048 cm^{-1}, which can be assigned to the ν_{assym} stretching vibration of the azide ligands. Similarly, a ν_{sym} stretching vibration of azide also appears at 1331 cm^{-1}. The above characteristic bands indicate the EO bridging mode of azide. Furthermore, the bands in the regions of 1645−1390 and 1270−750 cm^{-1} are observed as a result of the C−C and C−N stretching and bending modes of the tptz ligands.[17]

Structure Description of Complex 1. The X-ray structural analysis reveals that complex **1** is a 1D chain. The ORTEP diagram of the part of the chain with an atom-labeling scheme is shown in Figure 1. Here, the coordination sphere of each Mn^{II} center contains three N atoms (N26, N1, and N26*) of the chelating tptz ligand and four N atoms

(15) Spek, A. L. *PLATON, Molecular Geometry Program*; University of Utrecht: Utrecht, The Netherlands, 1999.

(16) Farrugia, L. J. ORTEP3 for Windows. *J. Appl. Crystallogr.* **1997**, *30*, 565.

(17) Nakamoto, K. *Infrared and Raman Spectra of Inorganic and Coordination Compounds*, 4th ed.; Wiley-Interscience: New York, 1986.

Figure 1. Coordination environment of Mn^{II} in **1** showing an atom-labeling scheme. Ellipsoids are at the 40% probability level. (Symmetry code: * = −*x*, *y*, $^3/_2$ − *z*; # = −*x*, −*y*, 2 − *z*; ## = *x*, −*y*, −$^1/_2$ + *z*.)

Table 2. Selected Bond Lengths (Å) and Bond Angles (deg) for Complex **1**^{a}

Mn1−N1	2.3135(18)	Mn1−N11	2.2716(13)
Mn1−N26	2.4305(13)	Mn1−N11#	2.2739(12)
N1−Mn1−N11	83.18(2)	Mn1#−N11−N12	128.00(9)
N1−Mn1−N26	67.91(3)	N11−N12−N13	179.36(13)
Mn1−N26−C21	118.35(8)	Mn1−N26−C25	124.70(9)
N1−Mn1−N11#	139.60(3)	N11−Mn1−N26	82.51(4)
N11−Mn1−N11*	166.36(4)	N11−Mn1−N26*	92.35(4)
N11−Mn1−N11#	73.84(4)	N11−Mn1−N11##	117.33(4)
N11*−Mn1−N26	92.35(4)	N26−Mn1−N26*	135.81(4)
N11#−Mn1−N26	138.11(4)	N11##−Mn1−N26	80.12(4)
N11*−Mn1−N26*	82.51(4)	N11*−Mn1−N11##	117.33(4)
Mn1−N11−N12	123.84(8)	N11#−Mn1−N26*	80.12(4)
N11##−Mn1−N26*	138.11(4)	N11#−Mn1−N11##	80.80(4)
Mn1−N1−C2	122.27(8)	Mn1−N11−Mn1#	106.16(4)

^{a} Symmetry code: * = −*x*, *y*, $^3/_2$ − *z*; # = −*x*, −*y*, 2 − *z*; ## = *x*, −*y*, −$^1/_2$ + *z*.

(N11, N11*, N11#, and N11##) from the bridging azide (Figure 1). Each Mn^{II} is connected to two other symmetry-related Mn^{II} centers via two doubly EO azide bridges, forming an infinite 1D chain along the crystallographic *c* axis. Thus, here the Mn^{II} ion shows an unusual 7 coordination number with a distorted pentagonal-bipyramidal geometry. The equatorial plane of the pentagon is formed by four N atoms of the bridging azido ligand and another N (N1) of the tptz ligand, whereas the axial coordination sites are occupied by two N atoms of the tptz ligand (N26 and N26*). Selected bond distances and angles are depicted in Table 2, which are comparable with other seven-coordinated Mn^{II} systems.[18] The Mn−N$_{azide}$ distances are 2.2716(13) and 2.2739(12) Å, whereas the Mn−N$_{tptz}$ distances range between

(18) (a) Karmakar, T. K.; Ghosh, B. K.; Usman, A.; Fun, H.-K.; Rivière, E.; Mallah, T.; Aromí, G.; Chandra, S. K. *Inorg. Chem.*, **2005**, *44*, 2391. (b) Deroche, A.; Morgenstern-Badarau, I.; Cesario, M.; Guilhem, J.; Keita, B.; Nadjo, L.; HoueeLevin, C. *J. Am. Chem. Soc.* **1996**, *118*, 4567. (c) Sra, A. K.; Sutter, J. P.; Guionneau, P.; Chasseau, D.; Yakhmi, J. V.; Kahn, O. *Inorg. Chim. Acta* **2000**, *300*, 77.
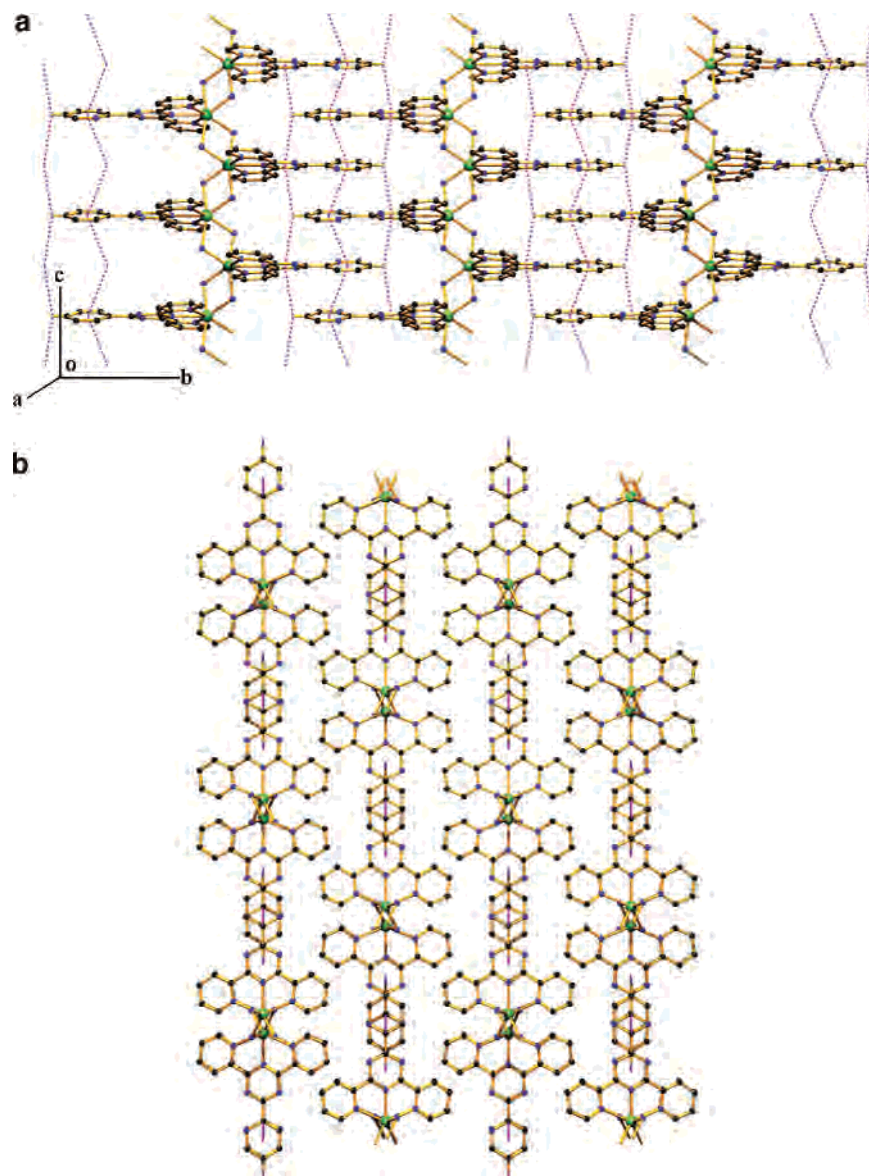
Figure 2. (a) Formation of a sheet by the locking of 1D [Mn(tptz)(N$_3$)$_2$]$_n$ chains with face-to-face $\pi-\pi$ interactions and C–H⋯π interactions (dotted magenta lines indicate $\pi-\pi$ and C–H⋯π interactions). H atoms (except the CH– of terminal pyridyl rings) and noncoordinated N(azide) atoms are omitted for clarity. (b) Disposition of the supramolecular sheets viewed along crystallographic c axis.
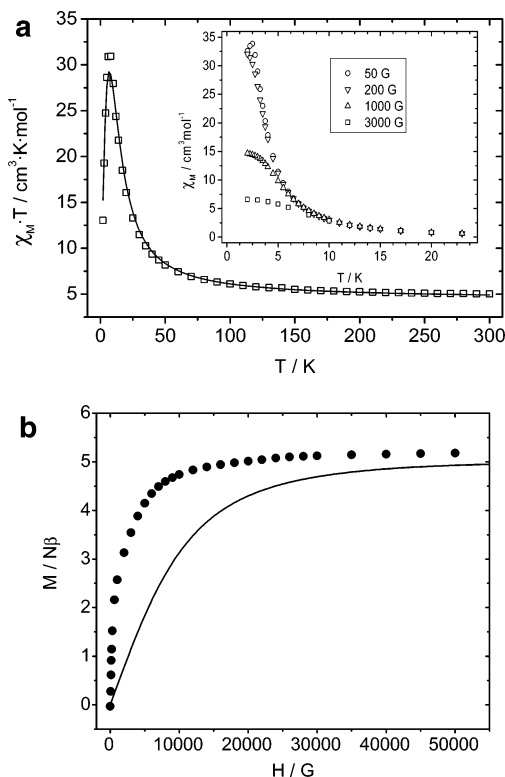
2.3135(18) and 2.4305(13) Å. The EO bridging azides that are linear show slightly asymmetric N–N distances. The Mn⋯Mn distance through the EO azide bridge is 3.634(1) Å, and Mn1–N11–Mn1# angle is 106.16(4)°, which lies within the range for Mn^{II} ions with the EO azide bridge.[6a]

The crystal packing of **1** indicates that the adjacent 1D chain orients the tptz ligand in such a way that the chains are interlocked by face-to-face $\pi-\pi$ interactions occurring between the pyridyl rings [R1 = N8–C7–N8*–C9*–C10–C9; R2 = C7–C8–C9–C10–C9*–N8* (* = −x, y, $^3/_2$ − z)] of tptz, having there centroid–centroid distances of 3.286-(1) Å. The $\pi-\pi$ interactions are quite strong because the dihedral angles between the rings are 0° whereas the slip angles are 22.97(1)° for all four interactions (table in the Supporting Information). The $\pi-\pi$ interactions are supplemented by the C–H⋯π interactions [C10–H10 to the triazine ring R3 = N1–C2–N3–C4–N3*–C2* (* = −x, y, $^3/_2$ − z)] with an H⋯R distance of 3.3654(1) Å and an C–H⋯R angle of 98.67(1)° to form a supramolecular 2D sheet (Figure 2).

Magnetic Study and Magnetostructural Correlation. The magnetic susceptibility of **1** was measured at 2−300 K with an external field of 3000 G. The $\chi_M T$ vs T plot (Figure 3a) indicates ferromagnetic coupling between the Mn^{II} centers bridged by the $\mu_{1,1}$-N$_3$ ligands. Indeed, $\chi_M T$ has a value of 5.07 cm^3 K mol^{-1} at 300 K, slightly higher than the expected value for an isolated octahedral Mn^{II} ion (4.38 cm^3 K mol^{-1} and TIP = 0). Indeed, in complex **1** the Mn^{II} ion is heptacoordinated; thus, there is a nonzero TIP value. $\chi_M T$ values increase gradually upon cooling to ca. 75 K. Below this temperature, $\chi_M T$ increases abruptly to a maximum value of 31.19 cm^3 K mol^{-1} at 8 K because of rapidly increasing ferromagnetic correlations between adjacent spin carriers. Upon cooling to 2 K, $\chi_M T$ decreases quickly to 13.19 cm^3 K mol^{-1} because of possible interchain antiferromagnetic interactions. The same behavior has been observed in other

Figure 4. Field-cooled magnetization vs temperature at applied fields of (from bottom to top) 15, 30, 50, 200, 1000, and 3000 G. The inset shows the magnetization curves at 15, 30, and 50 G with a maximum of $T_c = 2.7$ K. The solid lines joining the experimental points are just guides for the eye.

Figure 3. (a) Plot of $\chi_M T$ vs T of **1**. The solid line corresponds to the best fit (see the text). The χ_M vs T curves below 25 K at applied fields of 3000, 1000, 200, and 50 G are shown in the inset. (b) Plot of the reduced magnetization $M/N\beta$ vs applied field H at 2 K for **1**. The continuous line corresponds to the Brillouin function for an isolated $S = {}^5/_2$ with $g = 2.0$.

related complexes such as *trans*-[Mn(N$_3$)$_2$(pyz)]$_n$[19] (pyz = pyrazine) and *cis*-[Mn(N$_3$)$_2$(2-bzpy)]$_n$ (2-bzpy = 2-benzoylpyridine).[20] To determine the exchange parameters via a N$_3$ bridge type, $\chi_M T$ was fitted to the $S = {}^5/_2$ Fisher chain model,[21] χ_M (eq 1), in conjunction with an additional mean-field correction term, χ_{MF} (eq 2), where N is Avogadro's number, μ_B is the Bohr magneton, k_B is the Boltzmann constant, and z is the number of nearest neighbors. The best least-squares fit parameters gave $J = 4.07$ cm^{-1}, $zJ' = -0.13$ cm^{-1}, $g = 2.003$, $R = 5.22 \times 10^{-4} = \sum_i (\chi_M T_{cal} - \chi_M T_{obs})^2/(\chi_M T_{obs})^2$.
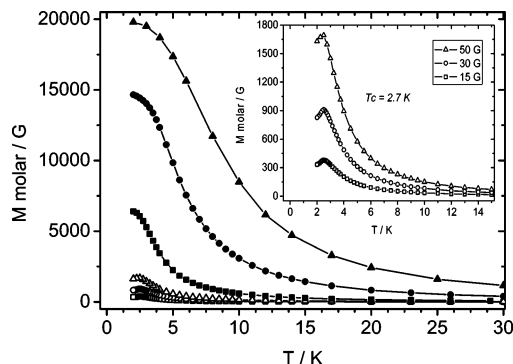
$$\chi_M = \left[\frac{Ng^2\mu_B^2 S(S+1)}{3k_B T}\right]\left[\frac{1+u}{1-u}\right] \quad (1)$$

where

$$u = \coth\left[\frac{JS(S+1)}{k_B T}\right] - \left[\frac{k_B T}{JS(S+1)}\right]$$

$$\chi_{MF} = \frac{\chi_M}{1 - \chi_M(zJ'/Ng^2\mu_B^2)} \quad (2)$$

The ferromagnetic coupling was confirmed by magnetization measurements performed at 2 K up to an external field

(19) Manson, J. L.; Arif, A. M.; Miller, J. S. *Chem. Commun.* **1999**, 1479.
(20) Abu-Youssef, M. A. M.; Escuer, A.; Gateschi, D.; Goher, M. A. S.; Mautner, F. A.; Vicente, R. *Inorg. Chem.* **1999**, *38*, 5716.
(21) Fisher, M. E. *Am. J. Phys.* **1964**, *32*, 343.

of 5 T showing the typical behavior of a soft ferromagnet because coercivity was not observed (Figure 3b). At higher field, the magnetization in $M/N\beta$ units indicates a saturated $S = {}^5/_2$ system, 5.18 $N\beta$. A comparison of the overall shape of the plot with the Brillouin plot for a fully isolated $S = {}^5/_2$ system indicates faster magnetization, consistent with the ferromagnetic interaction.

This ferromagnetic behavior may be explained by attending to the principal factors that influence the sign of the exchange interaction in the $[\{\mu_{1,1}\text{-N}_3\}_2\text{M}^{II}]$ system.[6] The magnetostructural correlation studies have shown a dependence of the ferromagnetic exchange coupling constant (J) on the M$-$N(azide)$-$M bridging angle. For Mn, the ferromagnetic exchange appears to increase with an increase of the bridging angle (starting from 100°) involved in the exchange pathway. Very recently, Aromí et al.[18a] have deduced from four dinuclear Mn^{II} compounds a linear relationship between the exchange integral (J) and the azide bridging angle (θ); $J = 0.64\theta - 64.5$. If this relationship holds for complex **1** [$\theta = 106.16(4)°$], a J value of ca. 3.43 cm^{-1} is anticipated. The experimental J value (4.07 cm^{-1}) appears to be close to the average among the prospective values using the previous relationship.

To characterize the magnetic transition from intrachain ferromagnetism to interchain antiferromagnetism of **1** in the low-temperature region, field-cooled magnetization was measured under different fields (Figure 4). At the lower field of 15, 30, and 50 G, the M vs T curve shows a maximum at ca. 2.7 K (Figure 4, inset), clearly indicating the occurrence of antiferromagnetic ordering of the ferromagnetic chains below the critical temperature. The magnetization maximum shifts toward low temperature as the applied field is increased to 200, 1000, and 3000 G. However, the magnetization at or above 200 G shows no maximum and tends to saturate at lower temperature, indicating that the interchain antiferromagnetic interactions are overcome by the external field. This behavior is characteristic of a metamagnet built of ferromagnetic chains.[22] The metamagnetic behavior is confirmed by the field dependence of magnetization (Figure 5). The sigmoidal shape of the $M/N\beta$ vs H curve at 2 K indicates the field-induced transition from an antiferromagnetic to a ferromagnetic state, which is characteristic of a metamagnet.
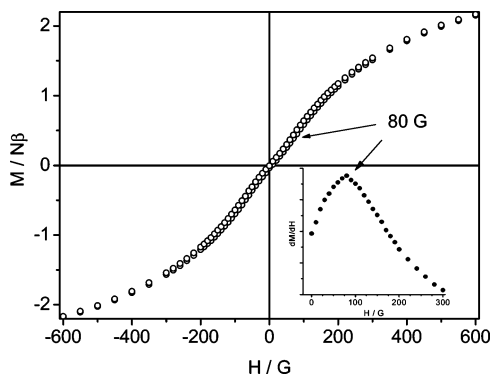
Figure 5. Hysteresis curve for **1**. The inset shows $\delta M/\delta H$ at low field.

The critical field is $\approx$80 G, estimated as the field at which a maximum $\delta M/\delta H$ value is reached (Figure 5, inset).

The temperature dependence of the ac magnetic susceptibility is also measured at zero dc field and confirms the occurrence of the magnetic transition with $T_c = 2.7$ K, at which the maximum of χ' (the in-phase component) occurs. The divergence of χ'' (the out-of-phase component) with the field starts at this temperature (Figure 6). This metamagnetic-like transition results from the presence of small antiferromagnetic interactions among the ferromagnetic chains and, in complex **1**, can be favored by the heptacoordination of the Mn ions.

Conclusion

From the above study, it can be concluded that, for the generation of new magnetic materials with azide ligands, the

(22) (a) Thompson, L. K.; Tandon, S. S.; Lloret, F.; Cano, J.; Julve, M. *Inorg. Chem.* **1997**, *36*, 3301 and references cited therein. (b) Toma, L. M.; Delgado, F. S.; Ruiz-Pérez, C.; Carrasco, R.; Cano, J.; Lloret, F.; Julve, M. *Dalton Trans.* **2004**, 2836. (c) Yoon, J. H.; Kim, H. C.; Hong, C. S. *Inorg. Chem.* **2005**, *44*, 7714.
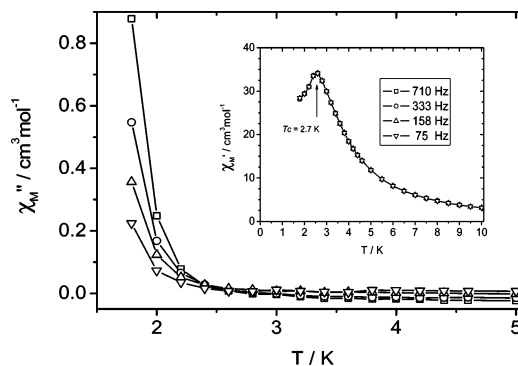
Figure 6. Real χ'_M (inset) and imaginary χ''_M parts of ac susceptibilities vs temperature at a dc field of $\sim$0 G and an ac field of 3.5 G for **1**. Frequencies from top to bottom are 75, 158, 333, and 710 Hz. The solid lines joining the experimental points are just guides for the eye.

choice of the metal atom and coligand is very important. Here it is shown that azide-bridged 1D chains are interdigitated by face-to-face $\pi-\pi$ and C—H$\cdots\pi$ interactions. From this fact, it can be attributed that the metamagnetic behavior may be due to the interchain weak interactions. Studies of these types of similar compounds are in progress, from which we are able to determine the role of weak interactions over the magnetic behavior of a molecule.

Supporting Information Available: X-ray crystallographic data in CIF format and a table of $\pi-\pi$ and C—H$\cdots\pi$ interactions in complex **1**. This material is available free of charge via the Internet at http://pubs.acs.org.

IC052088T